Frictional Properties of Surfactant-Coated Rod-Shaped Nanoparticles in Dry and Humid Dodecane

ARTICLE *in* THE JOURNAL OF PHYSICAL CHEMISTRY B · SEPTEMBER 2008

Impact Factor: 3.3 · DOI: 10.1021/jp802535j · Source: PubMed

5 AUTHORS, INCLUDING:

Mustafa Akbulut
Texas A&M University
41 PUBLICATIONS **922** CITATIONS
SEE PROFILE

Robert K Prud'homme
Princeton University
283 PUBLICATIONS **12,797** CITATIONS
SEE PROFILE

Yuval Golan
Ben-Gurion University of the Negev
126 PUBLICATIONS **2,580** CITATIONS
SEE PROFILE

Jacob Israelachvili
University of California, Santa Barbara
282 PUBLICATIONS **19,572** CITATIONS
SEE PROFILE

Frictional Properties of Surfactant-Coated Rod-Shaped Nanoparticles in Dry and Humid Dodecane†

Younjin Min,[⊥] Mustafa Akbulut,[§] Robert K. Prud'homme,[§] Yuval Golan,[‡] and Jacob Israelachvili*,[⊥]

Department of Chemical Engineering, University of California Santa Barbara, Santa Barbara, California 93106, Department of Chemical Engineering, Princeton University, A-306 Engineering Quadrangle, New Jersey 08544-5263, and Department of Materials Engineering and Ilse Katz Institute of Nanotechnology, Ben-Gurion University of the Negev, Beer-Sheva 84105, Israel

Received: March 24, 2008; Revised Manuscript Received: May 19, 2008

We have investigated the effects of humidity (water content or activity from 0 to ~0.98) on the frictional properties of surfactant-coated ZnS nanoparticles of various shapes, specifically, nanorods and nanowires, dispersed in an organic solvent (dodecane). The friction coefficients were found to be sensitive to even trace amounts of water, increasing logarithmically with time after the systems were exposed to humid air, doubling after 2−4 h of exposure time to air of relative humidity ~ 98%. We also show that increasing the humidity caused noticeable effects on the interactions of the nanoparticles, increasing their adhesion and aggregation through capillary forces. These effects should be considered in the design of organic solvents containing nanoparticles with physisorbed surfactants, for example, lube oils with nanoparticles additives, particularly those exposed to atmospheric conditions.

Introduction

Humidity and other environmental conditions significantly influence surface properties such as adhesion and friction because most surfaces have a physisorbed layer on them, except under ultrahigh vacuum.[1–4] For a hydrophilic surface, a monolayer or submonolayer of water will be present even at relatively low humidities, which can significantly affect the adhesion due to capillary forces and the friction due to "lubrication" forces.[5–7] Similarly, organic molecules can condense in and around the contact junctions of hydrophobic surfaces, which can significantly alter their friction forces.[8] When exposed to organic vapors or bulk organic liquids (oils), most surfaces, both hydrophobic and hydrophilic, bind a layer of the organic molecules sufficiently strongly that they do not easily come off when the surfaces are pressed or rubbed together. The surfaces never make direct contact,[9] which also protects them from becoming damaged. However, the presence of water can give rise to additional effects such as chemical changes and changes to the adhesion and friction of hydrophilic surfaces when water replaces the physisorbed layer of oil.

Most oil-based lubricant systems do not rely on the lubricating properties of the pure organic liquids, but contain various additives which typically include surfactant-coated nanoparticles chosen for both their physical and chemical properties. Previous research has shown that carbon nanotubes,[10–12] amorphous nanofilms,[13,14] and inorganic fullerene-like nanoparticles of WS_2 and MoS_2 sheets[15–20] can improve lubrication behavior. However, in the presence of water or when exposed to humid air, their frictional (lubrication) properties often deteriorate.[15,21,22]

Understanding the effect of the shape of "third-body" particles on friction and lubrication has always been an important tribological problem. Akbulut et al.[23–25] showed that surfactant-coated ZnS nanorods can provide both low friction and good surface-wear protection when used as additives in fluids that are not good lubricants on their own and measured friction coefficients of approximately 0.04 without damage over a large range of sliding speeds up to pressures of 200 MPa. They also showed that nanorods and nanowires perform better than nanospheres as lubricant additives. In this study, we investigated the effects of humidity on the friction and lubrication properties of nanorods and wires. We used a Surface Forces Apparatus (SFA) coupled with in situ multiple beam interferometry to measure and visualize these effects.

Experimental Methods

Tribological studies were carried out with a SFA equipped with a friction attachment where the upper surface was held with force-measuring springs and the lower surface was moved laterally at a uniform velocity by means of a piezoelectric "bimorph slider".[26] The resulting friction was measured from the deflection of the friction force-measuring spring system supporting the upper surface.[26]

The substrate surfaces were atomically smooth muscovite mica sheets, back silvered, and then glued onto cylindrical silica disks with Epon 1004 F glue (Shell Chemical Company, Houston, TX) where the back-silvered 500−550 Å thick Ag layers were used as the reflective layers for generating the interferometric fringes of equal chromatic order (FECO) needed to measure the geometry and separation of the two mica surfaces. This technique allows for the sliding surfaces to be imaged simultaneously as their nanoscale tribological parameters are measured and/or controlled. The typical shearing speeds V, back and forth sliding distances S, applied loads L, and pressures P were $V = 0.2-20$ μm/s, $S = 100-200$ μm, $L = 0-40$ mN, and $P = 0-10$ MPa.

† Part of the "Janos H. Fendler Memorial Issue".

* To whom correspondence should be addressed. E-mail: jacob@engineering.ucsb.edu.

[⊥] University of California Santa Barbara.

[§] Princeton University.

[‡] Ben-Gurion University of the Negev.

10.1021/jp802535j CCC: $40.75
Published on Web 08/15/2008

ZnS nanorods and nanowires were synthesized using the method described by Pradhan et al.[27] and were coated with the surfactant octadecylamine (ODA, $C_{16}H_{35}N$). The nanoparticles had ZnS core diameters of 1.0−1.5 nm and lengths of ∼8 and ∼200 nm for the rods and wires, respectively.

The nanoparticles were dispersed in *n*-dodecane in a nitrogen-purged dry glovebox. Typical nanoparticle concentrations were between 0.05 and 1 mg/ml. Molecular sieves (EM Science, type 4A, 8−12 mesh) were then added to the composite solutions to absorb any residual water. For the SFA experiments, a droplet of the appropriate dispersion was injected between two closely apposed mica surfaces, and the SFA chamber was gas-sealed in an atmosphere of dry nitrogen gas with a small Petri dish of phosphorus pentoxide (P_2O_5) powder to ensure complete dryness during the experiments. Dodecane was purchased from Sigma Aldrich and dried over molecular sieves prior to use. The relative humidity of the chamber was controlled by placing pure Milli-Q water or saturated aqueous solutions of lithium chloride (LiCl), potassium carbonate (K_2CO_3), or sodium chloride (NaCl) into the SFA chamber after removing the P_2O_5. Saturated LiCl, K_2CO_3, and NaCl solutions and pure Milli-Q water are known to give rise to an atmosphere with relative humidities (RH) of 11.3 ± 0.3, 43.2 ± 0.4, 75.3 ± 0.1, and ∼98%, respectively, at 25 °C.[24,28] Milli-Q water was purified by a MilliPore Gradient A10 system (Bedford, MA) and had a resistivity of ≥18.2 MΩ·cm and total organic content of ≤5 ppb. Phosphorus pentoxide and all salts were used as received from Fisher Scientific (Pittsburgh, PA).

Results

Effect of Humidity on the Forces in Dodecane without Nanoparticles. Before measuring the effects of water on the nanoparticles dispersions, "control" measurements were made on the forces between mica surfaces across pure dodecane liquid as a function of exposure time to humid atmospheres at 25 °C (Figure 1). When the surfaces were brought together in totally dry dodecane, only weak oscillatory forces were observed at distances below 2−3 nm with weak adhesive minima (cf. points • in Figure 1a and b), in agreement with previous measurements.[29] However, after introducing water (or humidity) into the atmosphere of the SFA chamber, the surfaces jumped in from increasingly larger distances into increasingly smaller distances of stronger adhesion, again as previously reported.[30–32] Thus, after ∼2 h of exposure, the adhesion force increased 50-fold to $F_{ad}/R \approx 210$ mN m^{-1}, which corresponds to an interfacial energy of $\gamma_i = F_{ad}/3\pi R \approx 22$ mJ m^{-2}. This increase in the adhesion force in the presence of water vapor has been shown to be due to the Laplace pressure arising from the capillary condensation of water around the mica−oil contact circle.[33]

Indeed, at medium to high humidity, surface-adsorbed and capillary-condensed water between and around the surfaces could be ascertained from the shapes of the FECO fringes, as illustrated in Figure 2. While no significant features were observed on the fringes at medium humidity (Figure 2a−c), Figure 2e shows the adsorbed water being squeezed out from between the surfaces as they are pulled together by the strong capillary (Laplace pressure) force, and Figure 2f shows the remains of the water bridge after the two surfaces have fully separated. The shift of the discontinuities on the fringes to shorter wavelengths (to the left) are indicative of small (∼10^{-9} μL or ∼1 μm^3) liquid lenses on the mica surfaces having a lower refractive index (i.e., water) than the surrounding medium (dodecane).[24,34]

The shapes of the FECO fringes in Figure 2e allowed us to estimate the growing water volume trapped between the surfaces

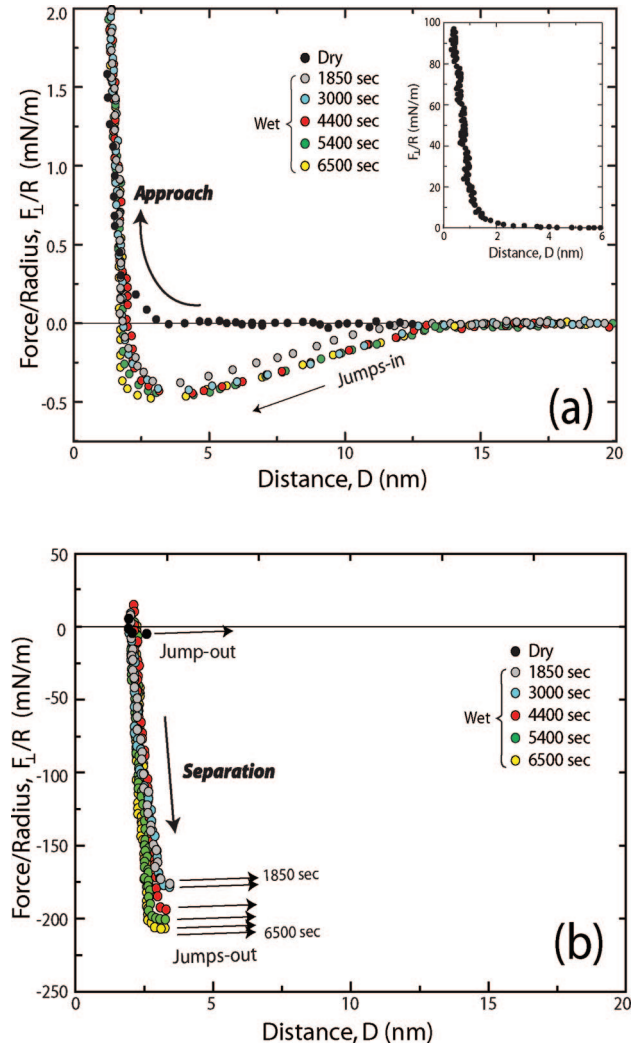

Figure 1. Normal forces $F_\perp$ between mica surfaces across dodecane as a function of substrate separation D with increasing exposure time to humid air at 25 °C. (a) Approach and (b) separation. The inset in (a) shows the maximum values of the repulsive oscillatory force barriers in the dry liquid.

as a function of time by measuring the surface separation (film thickness) D and contact area. The estimated water layer thicknesses per surface at different exposure times, t, are given in Table 1. These thicknesses correspond to trapped volumes of ∼1−4 μm^3, which are also consistent with the estimated volumes of the snapping bridges, mentioned above.

An increasing adhesion with increasing adsorbed water film thickness has previously been observed by Christenson and Israelachvili[35] in crude oil−mica systems under conditions of high humidity.

Effect of Humidity on the Friction of Forces Across Dodecane Containing Nanoparticles. Figure 3 shows the friction forces $F_{||}$ as a function of the normal load $F_\perp$ at increasing exposure times to humid vapor (RH ∼ 98%) for ZnS−ODA nanorods in dodecane at 25 °C. The friction forces roughly logarithmically increased with the exposure time. The dry friction was roughly linear with the load, and the "line" passed through the zero axes, as expected for such a nonadhesive system (known as Amontons's Law of Friction). In contrast, the humid friction was nonlinear and exhibited a finite friction already at zero load, indicative of an adhesion contribution to the friction force[9,36] and consistent with the expectation that the "humid" nanoparticles will adhere both to themselves and

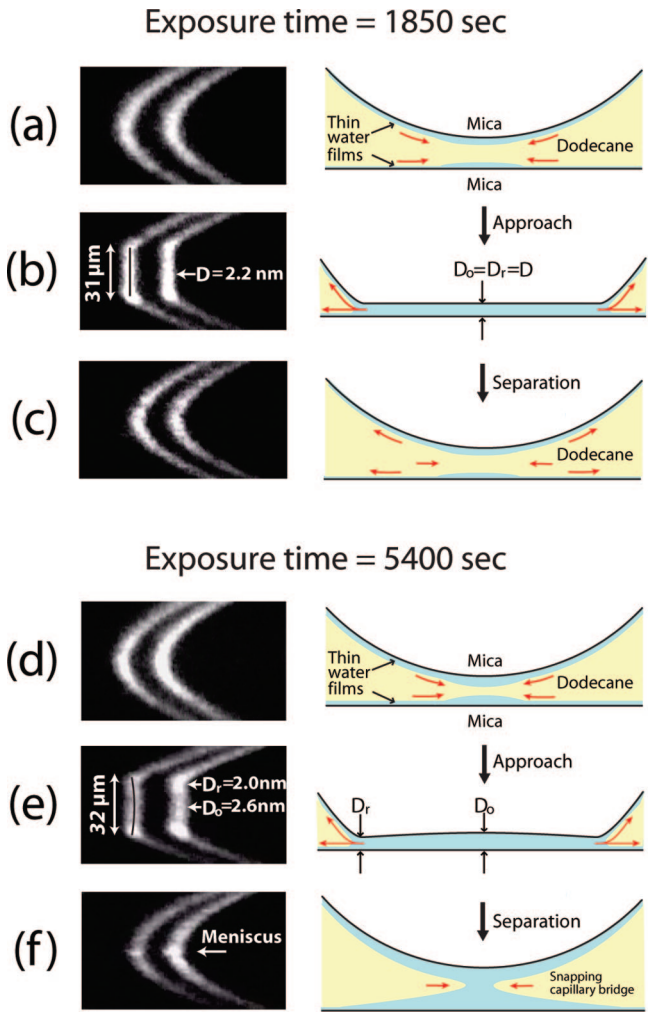

Figure 2. Representative FECO fringes (left) and corresponding schematics (right) showing the effects of a molecularly thin film of water on two mica surfaces as they approach each other in dodecane. (a, d) Approach and slight bulging of water film; (b, e) situation just after the surfaces have jumped into adhesive contact; note the higher water content in (e); (c, f) separation from the contact; (f) shows the snapping of the water bridge (meniscus), which disappears within a few minutes, returning the surfaces to their original state (d).

TABLE 1: Estimated Thickness of Adsorbed Water Per Mica Surface As a Function of Time of Exposure to Saturated Vapor

time of exposure (sec)	average water layer thickness (nm)	water volume (μm^3)
1850	2.2 ± 0.1	1.37
3000	2.2 ± 0.1	1.43
4400	2.2 ± 0.1	2.26
5400	2.3 ± 0.2	2.57
6500	2.3 ± 0.3	3.90

to the mica surfaces via capillary forces.[24] This is typical for adhesive junctions and is also expected from theories of friction where, in addition to the traditional linear term (for pure "load-controlled" friction), there is a term that varies with the contact area (the "adhesion-controlled" friction force) which can be calculated from the JKR (Johnson–Kendall–Roberts) theory of "contact mechanics"[37,38] if the "shear strength" is known. This contribution very much introduces a convex shape to the friction−load curve, as seen in Figure 3a for the wet (adhering) nanoparticles.

We also investigated the effects of humidity on the friction of ZnS−ODA nanowires. As can be seen in Figure 4, similar

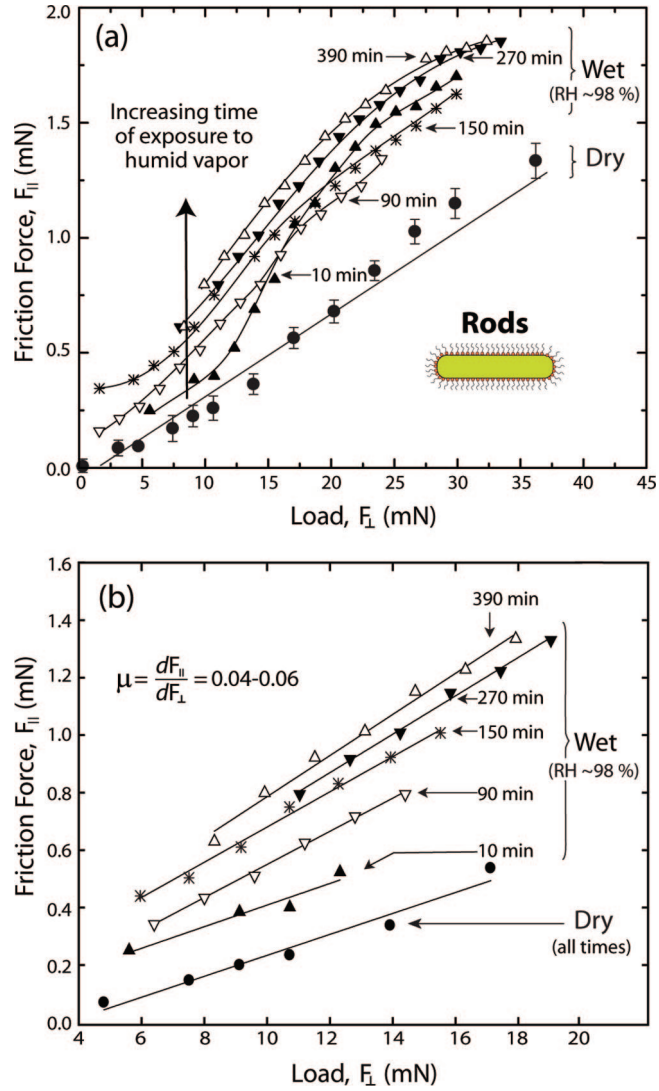

Figure 3. (a) Friction forces $F_{||}$ versus load $F_\perp$ as a function of exposure time to humid vapor (RH ~ 98%) and (b) their linear regimes. The concentration of the nanorods in dodecane was ~0.05 mg/ml, and the sliding velocity was 12.5 μm/s in both directions.

trends were observed showing the increased friction forces with increasing relative humidity conditions. However, both the friction forces and the friction coefficients were significantly higher than those in the nanorod systems at the same RH and loads. For example, after 3−5 h of exposure to humid vapor, the mean friction coefficient increased from ~0.2 to ~0.5, compared to an increase of 0.04−0.06 for the nanorods. Also, the friction coefficients were much more sensitive to the RH and equilibration time with the humid vapor.

Figure 5 shows the measured normal forces between mica surfaces across dodecane containing ZnS−ODA nanowires as a function of exposure time to humid vapor. In the early stages of exposure, up to ~8 h, both the repulsion and "hard wall" thickness increase with the exposure time. However, after about 1 day, the surfaces develop a long-range attraction that precedes the repulsion; see the curve after 20−24 h in Figure 5. This attraction can be attributed to the attractive capillary forces developed between the mica surfaces themselves in the presence of excess water,[24] which are superimposed on the existing repulsion between the surfaces across the trapped (aggregated) nanoparticles (see schematic Figure 7 later).

Interestingly, when the forces across the nanowire solutions exposed to different humidity conditions are compared at the

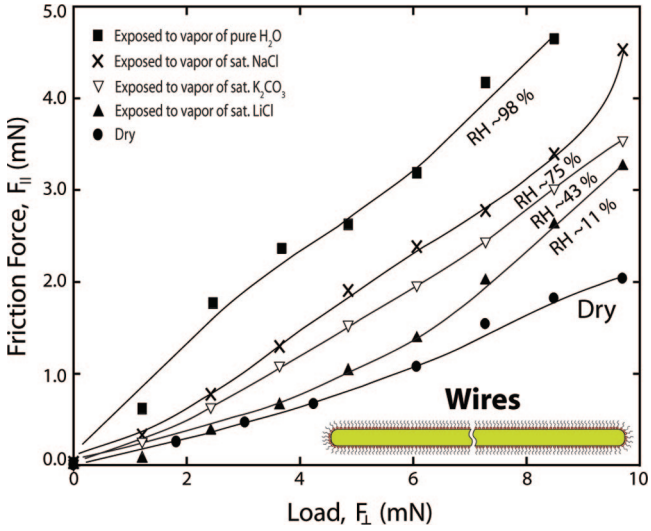

Figure 4. Friction forces $F_{||}$ versus load $F_{\perp}$ for mica surfaces sliding across 1 mg/mL nanowires in dry and wet dodecane at different relative humidities (RH) as shown after 3−5 h of equilibration with humid vapor. The sliding velocity was $V = 3.5\ \mu$m/s. We note that the friction forces had not yet saturated and were still increasing with time, albeit at a much reduced rate.

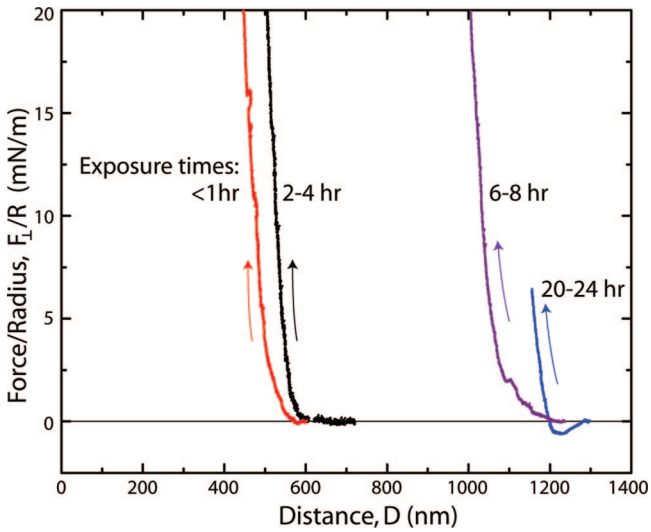

Figure 5. Normal forces $F_{\perp}$versus distance D between mica surfaces across 1 mg/mL ZnS−ODA nanowires in dodecane with increasing exposure time t to humid vapor (pure water, RH ~ 98%), as shown. The arrows indicate that the forces were measured upon approach; the forces measured upon separation (not shown) were very similar, indicating short-term reversibility, that is, "elastic-like" behavior, of the nanoparticle layers, which describes a system or material (a thin film in our case) that deforms linearly with the applied stress or load, whether applied normally or laterally. In the case of an elastic spring, it expands proportionally to the load, but the original shape (or spring length) is recovered when the stress or load is removed, known as reversible. Some systems are not perfectly elastic and therefore not reversible, but this may depend on the rates of loading and unloading or the length of time the system experiences the load. Thus, the system may return to its original state if the load is removed soon after it is applied (short-term reversibility) but not if it is applied for a long time.

same exposure times, the magnitude and range of the forces are the same, while the stronger, more repulsive shorter-ranged forces are the greatest for the two most humid vapors and the least for the least humid and dry vapors.

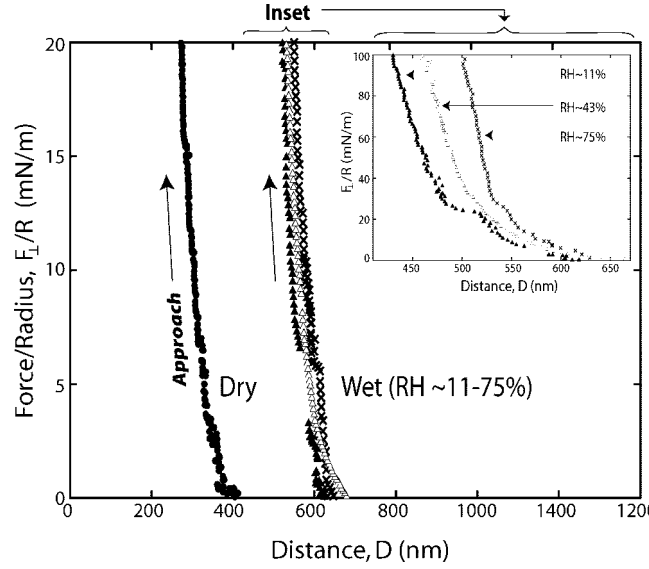

Figure 6. Normal forces $F_{\perp}$between mica surfaces as a function of mica−mica separation D measured at similar exposure times of 3−5 h of 1 mg/mL ZnS−ODA nanowires in dodecane exposed to vapors of different humidity conditions (RH).

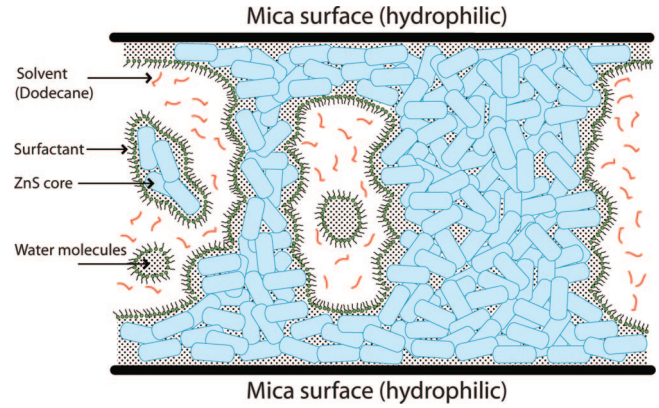

Figure 7. Schematic of the surface-coated ZnS cores in dodecane under near fully hydrated conditions. The surfactant molecules, which are initially physically bound to the ZnS cores, become separated from the cores as the humidity (water content) increases, causing the formation of water bridges.

Discussion

To better understand the effects of humidity on friction, we start by discussing the effects of water (humidity) on the normal forces. In dodecane exposed to humid vapor or in contact with bulk liquid water, the water initially diffuses into the dodecane (saturation concentration of 65 ppm by weight) and penetrates into the surfactant headgroup−nanoparticle core interface region, replacing the headgroup on the hydrophilic core surface by a thin water layer. At the same time, a water film also grows at the dodecane−mica interface. The rates of water penetration depend on the whole system—the volume of dodecane, the RH or activity of the water, and whether the water is introduced from vapor or from bulk aqueous solution.

Previous work on the interactions between surfactant monolayers physisorbed on (hydrophilic) mica, whether exposed to air or hydrocarbon liquids, has shown that water penetrates into the monolayer headgroup region, causing the surfactant molecules to become more fluid-like. A thin layer of interfacial water now separates the monolayer from the hydrophilic substrate surface. Eventually, the hydrophilic surfaces become

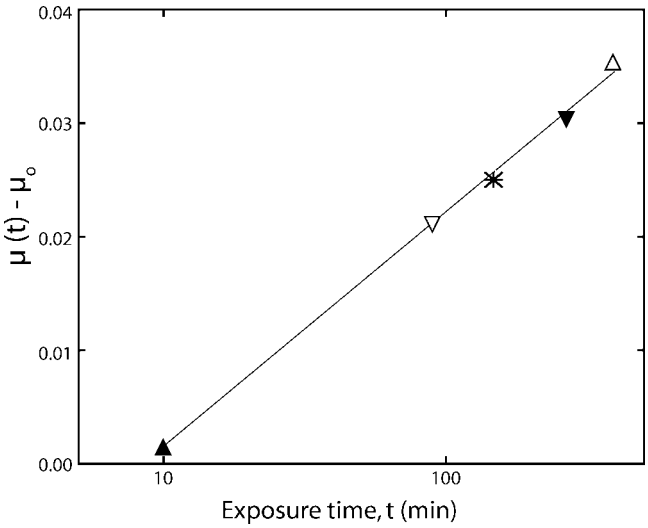

Figure 8. Increase in the friction coefficient versus (logarithmic) time of exposure to humid water vapor at RH ≈ 98% ($P_{vap}/P_{sat} = 0.98$) for the nanorod solutions of Figure 3b. The data cannot be fitted by a linear or log−log plot.

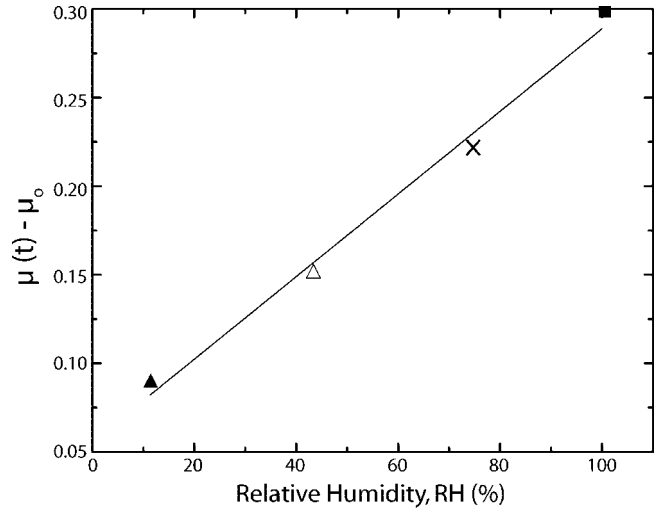

Figure 9. Change in the friction coefficient versus relative humidity for a given exposure time of $t = 250-350$ min for the nanowire system shown in Figure 4.

TABLE 2: Changes in the Friction Coefficient of Nanowires (Figure 4) as a Function of Relative Humidity after an Exposure Time of $t = 250-350$ min

sat solution	RH = 100(P_{vap}/P_{sat})	$\mu(t)$	$\Delta\mu = \mu(t) - \mu_0$
dry	~0	$0.22 = \mu_0$	0
LiCl	11.3	0.31	0.09
K_2CO_3	43.8	0.37	0.15
NaCl	75.3	0.44	0.22
pure water	~98	0.52	0.30

connected by water bridges which increase their adhesion through the strong capillary force generated by the condensation.[1,8,39–41] None of this occurs in totally dry conditions where the surfaces interact via the weak van der Waals and oscillatory "solvation" or "structural" forces across the pure *n*-alkane liquids. In wet conditions, the forces change to a monotonic, strongly attractive long-range force, as found in this study (cf. curve after 20−24 h in Figure 5), except that now there are additional forces between the surfaces due to the nanoparticles adsorbed on the surfaces and trapped between them.

Alig et al.[24] have shown that in a dry organic solvent, the hexadecylamine surfactant keeps the ZnS nanoparticles from aggregating due to the "screening" of the van der Waals forces by the surfactant chains, but they showed that aggregation occurs once water enters the solution, even just from the vapor where the relative humidity was estimated to be 94−98%. To understand the detailed mechanism of the humidity-induced aggregation of nanoparticles during confinement, they utilized a SFA and various chemical analyses such as X-ray photoelectron spectroscopy (XPS), infrared spectroscopy (IR), and UV−vis spectroscopy. XPS spectra showed that there was a narrowing in the $2P_{3/2}$ peak when the ZnS nanoparticles were exposed to water, suggesting either the removal of the surfactants or the partial oxidation of ZnS.[24] On the other hand, UV−vis spectroscopy showed that the locations of the absorbance peak for the humid and dry cases were not very different, that is, both stayed at about 290 nm. It is known that ZnS and ZnO of the same sized nanoparticles have very different absorbance peak locations in their UV−vis spectra, allowing these authors to conclude that there was negligible oxidation.[42] Comparison of the IR spectra among pure surfactant, surfactant-coated nanoparticles, and wet surfactant-coated nanoparticles indicated that (i) there is a N−H stretching peak at around 3100−3400 cm^{-1} for pure HDA that disappears when HDA is attached to the ZnS core but reappears after ZnS−HDA is exposed to water.[24] In the light of these results, Alig et al.[24] concluded that in the presence of water, the surfactant layer covering the ZnS cores is lifted or replaced by a layer or more of water. These findings should apply equally to our present experiments describing the shear (or frictional) forces of the nanoparticles.

Aggregation via capillary forces can therefore now occur, as previously also observed in a variety of nonaqueous liquids containing larger colloidal particles.[1,43] Aggregation via attractive van der Waals forces can also occur if the water simply removes the surfactant layer from the surface to form a water-in-oil microemulsion or swollen inverted micelles in the organic liquid.[44] Either of these explanations would be consistent with the data of Figures 1, 4, and 6, which reveal the slow growth of layers of aggregated nanoparticles on the surfaces that adhere to each other via capillary and/or enhanced van der Waals forces. Figure 6 appears to show that these layers have a more easily compressible outer region (Figure 6, main figure) and more rigid inner ones (Figure 6, inset), where the outer region is much less sensitive to the water content. It is possible that the nanowires in the outer regions of the adsorbed layers are less densely packed and randomly oriented and therefore give rise to a repulsive steric force that is determined by their elastic properties, while the inner regions have more compact and well-oriented water-bridged particles that are overall more rigid.[23]

Figure 7 is a schematic of the hydrated system. As more water goes into the dodecane solution where the nanoparticles are initially well dispersed, more water films build up at all interfaces to the point where the ZnS cores (and hydrophilic mica surfaces) are connected by water bridges, pulling all of the surfaces tightly together.[24]

The friction forces across the nanoparticle solutions increased with the water content, as previously observed with nonpolar liquids between hydrophilic surfaces,[45,46] and also increased noticeably with the exposure time. Both the friction coefficients, defined by, $dF_{||}/dF_{\perp}$, and the zero-load friction force increased with the RH and time, indicative of increasing adhesion of the nanoparticles and surfaces to each other.[8,47–49] A general expression for the friction force that includes both the nonadhesive load-dependent and adhesion-dependent contributions is[9]

$$F = S_c A + \mu L \quad (1)$$

where S_c is the adhesion-dependent critical shear stress and A is the (real) area of contact. Depending on whether the friction force in eq 1 is dominated by the first or second term, one may refer to the friction as adhesion- or load-controlled, respectively. In our system, in the presence of water, the friction force transforms from pure load-controlled friction to adhesion-controlled friction at low loads and a mixture of both at high loads.

Crassous et al.[50] developed an empirical equation to describe the observed time-dependent friction forces between two rough surfaces exposed to undersaturated water vapor:

$$\mu(t) \approx \mu_0 + \alpha(P_{vap}/P_{sat})\ln t \quad (2a)$$

or

$$\Delta\mu = \mu(t) - \mu_0 = \alpha(P_{vap}/P_{sat})\ln t \quad (2b)$$

where μ_0 is the friction coefficient under dry conditions and $\mu(t)$ is the time-dependent friction coefficient after an exposure time t to vapor of relative humidity P_{vap}/P_{sat}. Although this equation was obtained for unlubricated surfaces, it shows good agreement with our data, as shown in Figures 8 and 9 (however, since $\ln t$ is undefined at $t = 0$, where $\ln t = -\infty$, the data at zero times are not shown).

Figure 8 shows that $\Delta\mu \propto \log t$ for a given (constant) RH or P_{vap}/P_{sat} for the nanorod system studied. To further test eq 2 and the constancy of the factor α, a plot of $\Delta\mu$ versus P_{vap}/P_{sat} measured at the same (constant) time t should be a straight line with a slope of $\alpha \log t$. Table 2 gives the measured values of the relevant parameters for the nanowire system studied in Figure 4, and Figure 9 is a plot of $\Delta\mu$ versus RH at $t = 250-350$ min for this system, giving a line of approximately constant slope. The friction forces clearly increased linearly with the relative humidity for a given exposure time.

Conclusions

The frictional properties of nanoparticle additives composed of variously shaped surfactant-coated ZnS nanoparticles dispersed in organic solvent were found to be very sensitive to humidity. When the composite solution was exposed to even trace amounts of water, the friction forces increased noticeably with increasing time of exposure. This was attributed to changes in the normal forces in the presence of water. More specifically, the normal force (or load) increased due to the attractive Laplace pressure or capillary force generated by the condensation of water bridges. The change in the normal forces, in turn, affected the friction forces. This is an interesting example where the friction transformed from load-controlled to adhesion-controlled friction as the adhesion contribution to the friction force increased significantly. The friction results were found to be in good agreement with previous experiments and previous empirical models describing the effects of humidity on friction.

Our results also demonstrate that nanorods provide better lubrication properties than those of nanowires, where the latter exhibited twice the friction coefficients in both the dry and wet environments studied. This difference may be due to the easier sliding/shearing and possible rolling of short rods in confined layers. However, the humidity increased the friction coefficients in both systems, that is, regardless of the shape of the nanoparticles. These effects should be considered in the design of nanoparticle lubricants or lubricant/additive systems, especially those that operate under atmospheric or humid conditions.

Acknowledgment. We acknowledge Nataly Belman for synthesizing the nanoparticles. Y.G. and J.I. thank the U.S.−Israel Binational Science Foundation, Grant Number 2006032, and Y.M. thanks the MRSEC Program of the NSF under Award Number DMR05-20415 for substantially supporting this work.

References and Notes

(1) Chen, Y. L. E.; Gee, M. L.; Helm, C. A.; Israelachvili, J. N.; McGuiggan, P. M. *J. Phys. Chem.* **1989**, *93*, 7057–7059.
(2) Mazeran, P. E. *Mater. Sci. Eng., C* **2006**, *26*, 751–755.
(3) Lim, J. C.; Neuman, R. D.; Park, S. *Langmuir* **2002**, *18*, 6125–6132.
(4) Ruths, M.; Israelachvili, J. N.; Ploehn, H. J. *Macromolecules* **1997**, *30*, 3329–3339.
(5) Adams, M. J.; Briscoe, B. J.; Law, J. Y. C.; Luckham, P. F.; Williams, D. R. *Langmuir* **2001**, *17*, 6953–6960.
(6) Ando, Y. *Tribo. Lett.* **2005**, *19*, 29–36.
(7) Sirghi, L. *Appl. Phys. Lett.* **2003**, *82*, 3755–3757.
(8) Israelachvili, J.; Maeda, N.; Rosenberg, K. J.; Akbulut, M. *J. Mater. Res.* **2005**, *20*, 1952–1972.
(9) Bhushan, B. *Springer Handbook of Nanotechnology*; Springer-Verlag: New York, 2004.
(10) Cumings, J.; Zettl, A. *Science* **2000**, *289*, 602–604.
(11) Falvo, M. R.; Taylor, R. M.; Helser, A.; Chi, V.; Brooks, F. P.; Washburn, S.; Superfine, R. *Nature* **1999**, *397*, 236–238.
(12) Buldum, A.; Lu, J. P. *Phys. Rev. Lett.* **1999**, *83*, 5050–5053.
(13) Liu, Y.; Erdemir, A.; Meletis, E. I. *Surf. Coat. Technol.* **1996**, *82*, 48–56.
(14) Erdemir, A.; Switala, M.; Wei, R.; Wilbur, P. *Surf. Coat. Technol.* **1991**, *50*, 17–23.
(15) Chhowalla, M.; Amaratunga, G. A. J. *Nature* **2000**, *407*, 164–167.
(16) Rapoport, L.; Bilik, Y.; Feldman, Y.; Homyonfer, M.; Cohen, S. R.; Tenne, R. *Nature* **1997**, *387*, 791–793.
(17) Rapoport, L.; Leshchinsky, V.; Lapsker, I.; Volovik, Y.; Nepomnyashchy, O.; Lvovsky, M.; Popovitz-Biro, R.; Feldman, Y.; Tenne, R. *Wear* **2003**, *255*, 785–793.
(18) Golan, Y.; Drummond, C.; Homyonfer, M.; Feldman, Y.; Tenne, R.; Israelachvili, J. *Adv. Mater.* **1999**, *11*, 934-+
(19) Golan, Y.; Drummond, C.; Israelachvili, J.; Tenne, R. *Wear* **2000**, *245*, 190–195.
(20) Drummond, C.; Alcantar, N.; Israelachvili, J.; Tenne, R.; Golan, Y. *Adv. Funct. Mater.* **2001**, *11*, 348–354.
(21) Rapoport, L.; Leshchinsky, V.; Lvovsky, M.; Nepomnyashchy, O.; Volovik, Y.; Tenne, R. *Wear* **2002**, *252*, 518–527.
(22) Lancaster, J. K. *Tribo. Int.* **1990**, *23*, 371–389.
(23) Akbulut, M.; Alig, A. R. G.; Min, Y.; Belman, N.; Reynolds, M.; Golan, Y.; Israelachvili, J. *Langmuir* **2007**, *23*, 3961–3969.
(24) Alig, A. R. G.; Akbulut, M.; Golan, Y.; Israelachvili, J. *Adv. Funct. Mater.* **2006**, *16*, 2127–2134.
(25) Min, Y.; Akbulut, M.; Belman, N.; Golan, Y.; Zasadzinski, J.; Israelachvili, J. *Nano Lett.* **2008**, *8*, 246–252.
(26) Luengo, G.; Schmitt, F. J.; Hill, R.; Israelachvili, J. *Macromolecules* **1997**, *30*, 2482–2494.
(27) Pradhan, N.; Katz, B.; Efrima, S. *J. Phys. Chem. B* **2003**, *107*, 13843–13854.
(28) *CRC Handbook of Chemistry and Physics*, 88th ed.; Taylor & Francis Group: Oxford, U.K., 2007−2008.
(29) Christenson, H. K.; Gruen, D. W. R.; Horn, R. G.; Israelachvili, J. N. *J. Chem. Phys.* **1987**, *87*, 1834–1841.
(30) Christenson, H. K.; Blom, C. E. *J. Chem. Phys.* **1987**, *86*, 419–424.
(31) Christenson, H. K.; Fang, J.; Israelachvili, J. N. *Phys. Rev. B* **1989**, *39*, 11750–11754.
(32) Christenson, H. K. *J. Colloid Interface Sci.* **1985**, *104*, 234–249.
(33) Israelachvili, J. N. *Intermolecular and Surface Forces*, 2nd ed.; Academic Press: New York, 1991.
(34) Israelachvili, J. *J. Colloid Interface Sci.* **1973**, *44*, 259–272.
(35) Christenson, H. K.; Israelachvili, J. N. *J. Colloid Interface Sci.* **1987**, *119*, 194–202.
(36) Gao, J. P.; Luedtke, W. D.; Gourdon, D.; Ruths, M.; Israelachvili, J. N.; Landman, U. *J. Phys. Chem. B* **2004**, *108*, 3410–3425.
(37) Johnson, K. L. *Proc. R. Soc. London, Ser. A* **1997**, *453*, 163–179.
(38) Johnson, K. L.; Kendall, K.; Roberts, A. D. *Proc. R. Soc. London, Ser. A* **1971**, *324*, 301.
(39) Kohonen, M. M.; Christenson, H. K. *Langmuir* **2000**, *16*, 7285–7288.

(40) Chen, Y. L.; Xu, Z. H.; Israelachvili, J. *Langmuir* **1992**, *8*, 2966–2975.
(41) Gee, M. L.; McGuiggan, P. M.; Israelachvili, J. N.; Homola, A. M. *J. Chem. Phys.* **1990**, *93*, 1895–1906.
(42) Zorman, B.; Friesner, R. A. *J. Chem. Phys.* **2003**, *118*, 5937–5946.
(43) Chen, Y. L.; Xu, Z. H.; Israelachvili, J. *Langmuir* **1992**, *8*, 2966–2975.
(44) Israelachvili, J. *J. Vac. Sci. Technol., A* **1992**, *10*, 2961–2971.
(45) Christenson, H. K. *J. Dispersion Sci. Technol.* **1988**, *9*, 171–206.
(46) Horn, R. G.; Israelachvili, J. N. *J. Chem. Phys.* **1981**, *75*, 1400–1411.
(47) Opitz, A.; Ahmed, S. I. U.; Schaefer, J. A.; Scherge, M. *Surf. Sci.* **2002**, *504*, 199–207.
(48) Tian, F.; Xiao, X. D.; Loy, M. M. T.; Wang, C.; Bai, C. L. *Langmuir* **1999**, *15*, 244–249.
(49) Ohnishi, S.; Stewart, A. M. *Langmuir* **2002**, *18*, 6140–6146.
(50) Crassous, J.; Bocquet, L.; Ciliberto, S.; Laroche, C. *Europhys. Lett.* **1999**, *47*, 562–567.

JP802535J